Can imaginary instantaneous normal mode frequencies predict barriers to self-diffusion?

J. Daniel Gezelter, Eran Rabani, and B. J. Berne
Department of Chemistry and Center for Biomolecular Simulation, Columbia University, 3000 Broadway, New York, New York 10027

(Received 28 February 1997; accepted 18 June 1997)

We discuss whether or not local information on the potential energy surface embodied by the distribution of unstable instantaneous normal modes can be used to predict the hopping rates and barrier heights for Zwanzig's model of self-diffusion [R. Zwanzig, J. Chem. Phys. **79**, 4507 (1983)] in simple liquids. Results from a set of simulations of Lennard-Jones particles done at multiple temperatures and densities are presented. These simulations show that the theories which predict diffusive barrier heights from the distribution of imaginary frequencies are questionable. This discrepancy is due to the presence of imaginary frequency instantaneous normal modes which persist into the solid phase. Model systems are used to show that imaginary frequency instantaneous normal modes (and even those at the top of the barrier along that mode) are not necessarily indicators of diffusive barrier crossing as used in Zwanzig's model. These false barriers are shown to be the cause of all of the imaginary frequency zero-force modes in the solid as well as many of the imaginary frequency modes in the high-density super-cooled liquid. We therefore dispute their utility as predictors of barrier heights or hopping rates in related liquid systems. We also show that attempts to separate the modes that are truly diffusive from those with false barriers using a frequency cutoff or local information on the potential energy surface are not successful at removing all of the non-barrier modes. © *1997 American Institute of Physics.* [S0021-9606(97)50336-9]

I. INTRODUCTION

In his 1983 paper[1] on self-diffusion in liquids, Zwanzig proposed a model for diffusion which consisted of ''cells'' or basins in which the liquid's configuration oscillates until it suddenly finds a saddle point on the potential energy surface and jumps to another basin. This model was based on and supported by simulations done by Stillinger and Weber[2–5] in which the liquid configurations generated by molecular dynamics were quenched periodically by following the steepest descent path to the nearest local minima on the potential energy surface. Stillinger and Weber found that as their simulations progressed, the quenched configurations were stable for short periods of time and then suddenly jumped (with some re-crossing) to other configurations.[3]

Zwanzig's model predicts the diffusion constant using τ, the lifetime which characterizes the distribution of survival times ($\exp(-t/\tau)$) in the various basins, and $\rho_q(\omega)$, the distribution of normal mode frequencies in the nearest basin (or *quenched* configuration). His diffusion constant can be expressed as

$$D=\frac{kT}{M}\int d\omega\rho_q(\omega)\frac{\tau}{(1+\omega^2\tau^2)}, \tag{1}$$

where M is the mass of the particles. Zwanzig used the Debye spectrum for $\rho_q(\omega)$ and estimated τ from the longitudinal and shear viscosities of the liquid.

Keyes has proposed a further elaboration of Zwanzig's basin-hopping model.[6] Keyes' contribution is a link between the hopping times between basins and the density of states of unstable instantaneous normal modes (INMs). INMs have been applied to many aspects of liquid and protein theory including Raman spectra,[7,8] rotational motion in molecular fluids,[9] friction,[10] the glass transition,[11,12] cluster dynamics,[13,14] and as a probe of barrier height distributions in peptides.[15,16]

In this paper we focus on the appropriateness of INMs for computing diffusion constants in simple liquids (both super-cooled and normal). We give evidence of the lack of validity of many of the key assumptions of the INM theory.[6] This evidence also undermines some of the more recent theories which use subsets of the imaginary frequency INMs.[11,12,17] First we review the major ideas contributing to these theories and then we subject each of them to tests against molecular dynamics simulations.

A. Instantaneous normal modes

The potential energy of the system at time t can be approximated as a Taylor series expansion of the potential around the configuration at $t=0$,

$$V(\mathbf{r}(t))\approx V(\mathbf{r}(0))-\mathbf{F}\cdot(\mathbf{r}(t)-\mathbf{r}(0)) + \frac{1}{2}(\mathbf{r}(t)-\mathbf{r}(0))^T\cdot\mathbf{D}\cdot(\mathbf{r}(t)-\mathbf{r}(0)), \tag{2}$$

where $\mathbf{r}(t)$ is the vector of mass-weighted Cartesian coordinates at time t, $\mathbf{F}$ is the gradient of the potential in these coordinates at $t=0$,

$$F_i=-\left.\frac{\partial V}{\partial r_i}\right|_{\mathbf{r}(0)}, \tag{3}$$

and $\mathbf{D}$ is the Hessian

$$D_{ij}=\left.\frac{\partial^2 V}{\partial r_i \partial r_j}\right|_{\mathbf{r}(0)}. \tag{4}$$

Since the configuration is chosen from a trajectory of the system at nonzero temperature, it will not necessarily be a minimum on the potential energy surface. Therefore, the force vector, **F**, will not necessarily vanish and the Hessian, **D**, is not necessarily positive definite.

Using a unitary transformation (**U**) that diagonalizes **D**, one can describe the potential energy surface and the short time dynamics based on motion along the (uncoupled) instantaneous normal modes. The potential energy surface can then be written as a sum over the instantaneous normal modes of the potential at $t=0$,

$$V(\mathbf{r}(t))\approx V(\mathbf{r}(0))+\sum_{\alpha}\left\{-f_\alpha q_\alpha(t)+\frac{1}{2}\omega_\alpha^2 q_\alpha^2(t)\right\}, \tag{5}$$

where the instantaneous normal mode coordinates, $q_\alpha(t)$, the forces, f_α, and frequencies, ω_α are related to the Cartesian coordinates by the same unitary transformation:

$$\begin{aligned} q_\alpha(t)&=[\mathbf{U}\cdot(\mathbf{r}(t)-\mathbf{r}(0))]_\alpha,\\ f_\alpha&=[\mathbf{U}\cdot\mathbf{F}]_\alpha,\\ \omega_\alpha^2&=[\mathbf{U}^T\cdot\mathbf{D}\cdot\mathbf{U}]_{\alpha\alpha}. \end{aligned} \tag{6}$$

B. Diffusion via the imaginary frequency INMs

In Keyes' work, the primary quantity of interest is the configuration-averaged density of states of the INMs, $\langle\rho(\omega)\rangle$, which is typically represented with the imaginary frequency branch plotted along the negative ω axis. Keyes represents the overall density of states as the sum of two parts,

$$\langle\rho(\omega)\rangle=\langle\rho_s(\omega)\rangle+\langle\rho_u(\omega)\rangle, \tag{7}$$

where the subscript s denotes the stable or positive frequency modes, and subscript u denotes the unstable or imaginary frequency modes.

Keyes' theory of diffusion connects $\langle\rho_u(\omega;T)\rangle$ and $\Omega_h=2\pi/\tau$, the average hopping rate between the basins of the Zwanzig model [Eq. (1)]. This connection rests on a number of assumptions.

The first assumption is that the hopping rate out of a given well is adequately described by transition state theory

$$\omega_h=\left(\frac{\omega_{well}}{2\pi}\right)\frac{Q_{barr}}{Q_{well}}e^{-\beta\Delta E(\omega)}, \tag{8}$$

where ω_{well} is the characteristic frequency in the well, ΔE is the difference in energy between the well and barrier region and Q_{barr}/Q_{well} is the ratio between the partition functions at the barrier and well region (excluding the reaction coordinate).

The average hopping rate, Ω_h, is then estimated by taking the sum over the s open exit channels from a given minimum and averaging over the different well regions:[6]

$$\Omega_h=\int_0^\infty d\omega\,\frac{\omega_{well}}{2\pi}sn(\omega)\frac{Q_{barr}}{Q_{well}}\langle e^{-\beta\Delta E(\omega)}\rangle, \tag{9}$$

where $n(\omega)$ is the normalized distribution of saddle frequencies about a given well.[18]

The second major assumption is that the barrier heights are a function of the frequencies of the unstable modes. To obtain this functional dependence, Keyes first derives $S(\omega;T)$, the relative likelihood that the system is in a barrier region with frequency ω instead of one of the well regions. $S(\omega;T)$ is obtained by summing the volume in configuration space surrounding each barrier region with frequency ω and dividing by the volume surrounding the well regions. The double summation is carried out by first summing over all well regions, and then summing over all barrier regions connected to each minimum. This procedure over-counts the barrier regions, but the over-counting can be corrected with a simple multiplicative factor. $S(\omega;T)$ is estimated as

$$S(\omega;T)=\left(\frac{s}{m}\right)\frac{Q_{barr}}{Q_{well}}n(\omega)\langle e^{-\beta\Delta E}\rangle. \tag{10}$$

Here s is again the number of barrier regions per well and m is the number of wells per barrier. To simplify, Keyes assumes that all minima are equivalent and thus assigns single values of s and m to the entire potential energy surface. In this approximation, the ratio s/m is a fixed value,[6] but Keyes does not connect the value of m to the INM density of states, so m remains a free parameter in the theory. Although m is a free parameter, it does have a physical meaning which limits the values it can take. m must be an integer, and must have a value larger than 1.

If the system visits a collection of barrier regions each with imaginary frequency ω, the density of unstable modes at that frequency is estimated to be

$$\langle\rho_u(\omega;T)\rangle\sim S(\omega;T)\left[1+\int d\omega S(\omega;T)\right]^{-1}, \tag{11}$$

where the term in square brackets normalizes over the entire configuration space (including both well and barrier regions). Readers interested in the full details of the derivation of $S(\omega;T)$ and how it relates to $\langle\rho_u(\omega;T)\rangle$ should consult Refs. 6 and 18.

Keyes third assumption is that the barrier heights obtained via the instantaneous normal mode (INM) frequencies [Eqs. (10) and (11)] are the same barriers to diffusion used in the transition state theory expression [Eqs. (8) and (9)], i.e., that the barriers obtained by a local expansion of the potential energy surface are the same barriers that lead to diffusion. Investigating the validity of this assumption is the primary aim of this paper, and we will pursue it in greater detail in section III.

An observation of the T and ω dependence of $\langle\rho_u(\omega;T)\rangle$ allows Keyes to fit the distribution with the functional form

$$\langle\rho_u(\omega;T)\rangle=a(T)\omega e^{-c\omega^4/T^2}. \tag{12}$$

Fitting this distribution over a range of temperatures results in an estimate for the hopping time[6]

$$\Omega_h = \frac{mc_2}{2\pi}\int_0^\infty d\omega \frac{\omega}{a(T)}\langle \rho_u(\omega;T)\rangle, \tag{13}$$

where c_2 is obtained from a fit using the functional form $a(T)=c_1-c_2 f_u(T)$ where $f_u(T)=\int d\omega \langle \rho_u(\omega;T)\rangle$ is the fraction of imaginary INMs.

Keyes approximates the distribution of quenched frequencies [$\rho_q(\omega)$ in Eq. (1)] for the Zwanzig theory by the following functional form,

$$\rho_q = \left[1-\cos\left(\frac{\pi\omega}{\omega_s}\right)\right](2\omega_s)^{-1}, \tag{14}$$

where ω_s is the peak frequency of the stable mode density of states ($\langle \rho_s(\omega)\rangle$).

The result of Keyes' work is a theory for the rate of self-diffusion that is based on local information about the potential energy surface obtained from only a few trajectories. The information required for his theory is static and can be obtained without any dynamical information via Monte Carlo or random walk techniques.[19] This would be the case for any theory in which all dynamical information is derived from transition state theory. If the assumptions underlying the connection between the imaginary mode density of states and the diffusion constant are correct, this represents a substantial contribution to our understanding of the process of diffusion in liquids.

C. Modifications to correct for anharmonicities

Vijayadamodar and Nitzan improved upon Keyes' theory by limiting the imaginary INMs included in $\langle \rho_u\rangle$ to those which have *zero force*.[17] A zero-force instantaneous normal mode (ZF-INM) is one for which $|f_\alpha| < |\omega_\alpha^2 \sigma\delta|$ where δ is a small constant and σ is the length scale used in the Lennard Jones potential energy surface [Eq. (18) below]. δ is chosen small enough so that N_0/δ is independent of δ (here N_0 is the number of modes that match the zero-force criterion). The prime goal of the Vijayadamodar and Nitzan paper was to eliminate the contribution of the imaginary INMs which are not unstable INMs. In other words, they wish to include only the contributions from imaginary INMs that are near the top of a barrier.

Vijayadamodar and Nitzan have used two routes to obtain the hopping rate. The first is based on Keyes' analysis, but using the zero-force INMs instead of the full INM density. Even though the barrier height distribution is quite different from Keyes' work, the calculated self-diffusion constants are similar for the two theories. Their approach still assumes that the barriers measured by the ZF-INMs are the same barriers to diffusion used in Zwanzig's theory of self-diffusion.

Next, Vijayadamodar and Nitzan proposed a ''naive'' model which assumes that every unstable zero-force INM arises from a symmetric double-well potential where $\omega^2_{barrier} = -\omega^2_{minima}$. A rate for crossing the barrier connecting the two identical wells was calculated from transition state theory. Once again, the calculated rates for self-diffusion are essentially identical to those obtained by Keyes.

Bembenek and Laird[11,12] have suggested a method that is very similar in character to the ideas in the Vijayadamodar and Nitzan paper. In their approach, the potential energy is calculated as the system is deformed along the projections of each instantaneous normal mode, and those modes which have two minima in their projected potential energy surfaces are called ''unstable'' or double-well (DW) modes. They suggest that the diffusion constant should be calculated using only those modes which have double wells. They have also classified the unstable or DW modes into ''extended'' or ''localized'' modes depending on the fraction of atoms that participate in the projected motion along that mode. Their measure of this fraction is the participation ratio,

$$p_\alpha \equiv \left[N\sum_{i=1}^{N} (\mathbf{e}_\alpha^i \cdot \mathbf{e}_\alpha^i)^2\right]^{-1}, \tag{15}$$

where $\mathbf{e}_\alpha$ is the normalized eigenvector corresponding to mode α. An extended mode (α) is one in which the participation ratio (p_α) is larger than a critical value. Bembenek and Laird have studied p_α as a function of the size of the system and (for $\rho^*=1$) were able to determine that the critical participation ratio separating extended from local modes was 0.4.[12] At other densities, it is conceivable that the participation ratio that separates extended from localized modes would have a different value, but Bembenek and Laird use the same cutoff ($p_\alpha = 0.4$) for different potential energy functions, so we do not expect the cutoff to be appreciably different at lower densities. Bembenek and Laird conclude that at temperatures below the glass transition (T_g), only the localized modes contribute to the distribution of unstable or DW modes, and that in the super-cooled liquids, the *extended* modes are the primary contribution to diffusive motion.

The distribution of DW modes is a *superset* of the imaginary frequency ZF-INMs proposed by Vijayadamodar and Nitzan, and either of these three distributions (full-INM, ZF-INM, or DW-INM) can be used for $\langle \rho_u(\omega)\rangle$ in Keyes' theory. The imaginary frequency zero-force modes enforce proximity to a barrier more strictly than the DW modes (since they require the current configuration to be on top of the saddle point along that mode), so one would expect them to be more useful at removing the non-barrier anharmonicities. The zero-force INMs have the added advantage of falling out of the INM computation with a trivial amount of additional computational work.

D. Other INM approaches to diffusion

Adams and Stratt[13,14] follow a somewhat more traditional approach to calculating the self-diffusion constant based on short time information. Their method is based on calculating the n^{th}-order moments of the velocity autocorrelation function (up to $n=4$) from the *stable* INM frequencies

$$C(t) = 1 - At^2 + Bt^4 + \cdots. \tag{16}$$

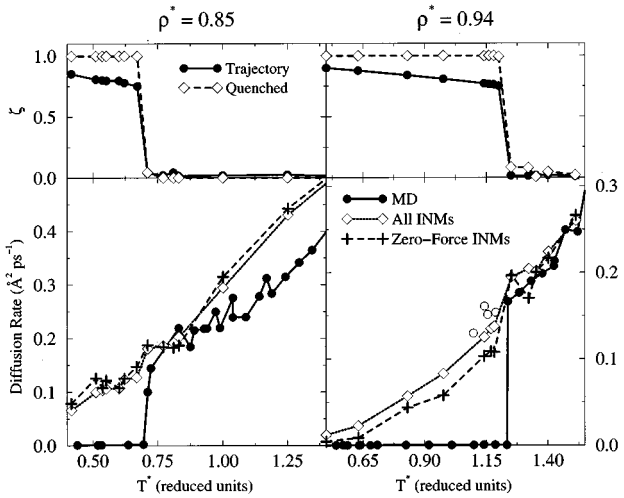

FIG. 1. Plots of the temperature dependence of the translational order parameter and the diffusion constant at 2 different densities. The left and right sides of the plot are for reduced densities ($\rho^*=\rho\sigma^3$) of 0.85 and 0.94, respectively. The top panels show the translational order parameter calculated for the raw trajectories (solid lines) and for quenched trajectories (dotted lines). In the bottom two panels, the closed circles (●) are the diffusion constants calculated via the Einstein relation [Eq. (17)], the diamonds (◇) are obtained using Keyes' theory, and the crosses (+) are calculated with the modifications in Ref. 17. The open circles (○) are results from simulations done on super-cooled liquids.

The full time dependence of the velocity autocorrelation function is then estimated using an interpolation introduced by Isbister *et al.*[20] and recently used by Egorov *et al.* for computing vibrational relaxation times.[21] This interpolation allows for analytic integration of $C(t)$ in the common expression for the diffusion constant,[22,23] and is a variant of procedures outlined almost three decades ago by Berne and Harp.[24]

In section II of this paper, we present results of simulations done near the melting temperatures of systems of 108 Lennard-Jones particles at a number of different densities. We have calculated the diffusion constants using Keyes' theory as well as with the Vijayadamodar and Nitzan modifications to the theory and compared them with the diffusion constants calculated via the Einstein relation[25]

$$D=\lim_{t\to\infty}\frac{1}{6t}\langle|\mathbf{r}_i(t)-\mathbf{r}_i(0)|^2\rangle, \tag{17}$$

where $\mathbf{r}_i(t)$ is the position of particle i at time t. In section III we report our investigation of the origin of the imaginary frequency instantaneous normal modes in solids and liquids composed of Lennard-Jones particles. Section IV contains our conclusions.

II. DIFFUSION CONSTANTS OF LENNARD-JONES LIQUIDS AND SOLIDS

We performed molecular dynamics simulations on systems of 108 particles interacting via the Lennard-Jones potential

$$V(r)=4\epsilon\left[\left(\frac{\sigma}{r}\right)^{12}-\left(\frac{\sigma}{r}\right)^{6}\right]-V_{cut}, \tag{18}$$

with parameters chosen to approximate the interactions between argon atoms ($\epsilon=0.238122$ kcal/mol, $\sigma=3.405$ Å).[26,27] V_{cut} is the standard Lennard-Jones potential evaluated at the cutoff radius ($r_{cut}=10$ Å) outside of which the potential energy is set to 0. The solid simulations were started from the face-centered cubic (fcc) lattice configuration with a total kinetic energy that was twice the target temperature of the simulation. The liquid simulations were also started in the fcc configuration, but with a kinetic energy that yielded an equilibrated temperature approximately twice the melting temperature. After a 50 ps period of equilibration, the velocities were scaled repeatedly until the trajectory was within 10 K of the target temperature. Another 50 ps period of equilibration followed the last velocity scaling, and 200 ps data collection runs began at the end of the equilibration. Diffusion constants were calculated via the Einstein relation during a longer (500 ps) run.

During the trajectory calculations, we accumulated the instantaneous normal mode frequencies every 1.2 ps and used them to calculate diffusion constants using Keyes' theory and the zero-force extension to his work.

Diffusion constants for the two INM-based theories have been plotted along with diffusion constants calculated via the Einstein relation [Eq. (17)] in the bottom panels of figure 1. In both INM-based theories we have adjusted the free parameter to match the computed self-diffusion constant at the higher density. The diffusion constants calculated via the Einstein relation are essentially zero for temperatures below the melting point. At temperatures just above the melting temperature, both INM-based theories do quite well at predicting the diffusion constant in the high density fluid, but neither of the INM-based theories predicts the sudden drop in the diffusion constant below the melting temperature for either of the two densities that we studied. Note that the data presented in figure 1 are obtained from constant energy trajectories, so the largest uncertainties are along the temperature axis. The data points each have a standard error of 0.06 in reduced temperature units along this axis.

Paralleling the trajectory calculations, we also acquired data for ''quenched'' trajectories. Every 10 fs, we followed the steepest descent path from the current configuration on the real trajectory to the nearest local minimum. This technique was first explored by Stillinger and Weber,[2–5] and led to Zwanzig's basin-hopping model.[1] We tracked the quenched configurations in order to learn more about the basins that are visited by liquids and solids at similar temperatures.

In order to ascertain whether a given trajectory was in the liquid or solid phase, we computed the translational order parameter,

$$\zeta(k)=\left\langle\left[\left(\frac{1}{N}\sum_{i=1}^{N}\cos(\mathbf{k}\cdot\mathbf{r}_i)\right)^2+\left(\frac{1}{N}\sum_{i=1}^{N}\sin(\mathbf{k}\cdot\mathbf{r}_i)\right)^2\right]^{\frac{1}{2}}\right\rangle, \tag{19}$$

where $\mathbf{k}$ is a reciprocal lattice vector of the initial fcc configuration. In our case, $\mathbf{k}=(2\pi/A)(-1,1,-1)$, where A is the size of a unit-cell of the original fcc lattice. We averaged the translational order parameter over a sample of statistically-independent configurations from both the raw trajectory and the quenched configurations. The calculated translational order parameters, ζ and ζ_q, are shown in the top panels of figure 1. At a reduced density $\rho^*=0.85$, the melting temperature $T^*\approx 0.69$ and at $\rho^*=0.94$, the melting temperature $T^*\approx 1.2$.

Particularly interesting is the fact that the quenched configurations of the solids all display a translational order parameter (ζ_q) of near unit value. This implies that from any configuration along the trajectories for a solid, the nearest local minimum is the defect-free original fcc lattice configuration. The order parameters for the liquids do not show any appreciable difference when comparing the regular and quenched trajectories.

The discrepancies between the simulated self-diffusion constant and those calculated with the INM theories in the solids led us to wonder whether primary quantities used in both INM theories (the INM density of states, $\langle\rho(\omega)\rangle$, and the zero-force INM density of states, $\langle\rho_0(\omega)\rangle$) change in any noticeable way as the temperature traverses the melting point. The densities of states for representative solids and liquids are plotted in figure 2. At identical densities, and at temperatures separated by only a few degrees, neither $\langle\rho(\omega)\rangle$ or $\langle\rho_0(\omega)\rangle$ display any obvious difference that would enable one to predict the phase from the spectrum.

The INM density of states, $\langle\rho(\omega)\rangle$, is used to compute the derived quantities f_u and $a(T)$ in Keyes' theory. In the upper panel of figure 3 we have plotted the fraction of unstable modes f_u at several temperatures near the solid-liquid phase transition. The fraction of unstable modes possesses a small discontinuity near the phase transition temperature. The discontinuity is also present in the multiplicative prefactor $a(T)$ [Eq. (12)] shown in the bottom panel of figure 3. Both $a(T)$ and f_u are the dominant parameters in Keyes' theory of diffusion. Therefore, one expects to find a discontinuity in the self-diffusion constant when going from the liquid to the solid, yet this discontinuity is much smaller in the predicted diffusion constants than it is in the temperature dependence of the real diffusion constant.

Of particular interest in figures 2 and 3 is the presence of the imaginary frequency INMs (and imaginary frequency zero-force INMs) in the *solids*. The quenched trajectories in the solids all lead to the fcc structure and the diffusion constants are essentially zero because there are no defects in the solids, so it is clear that no diffusive barriers are being crossed. Moreover, the projection of the full potential energy surface along some of the imaginary INMs has a double-well structure, yet quenching the system from both sides of the barrier results in the same defect-free fcc configuration. This leads us to question whether imaginary frequencies observed in solids (or liquids) are really giving us information about the barriers to diffusion.

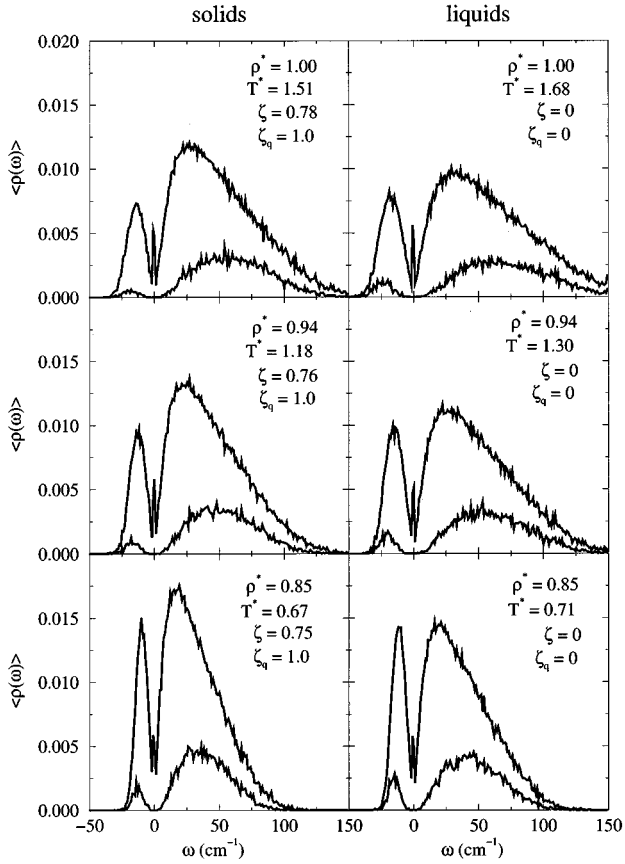

FIG. 2. The instantaneous normal mode density of states $\langle\rho(\omega)\rangle$ (plotted with the imaginary frequency branch on the negative ω axis) for a series of liquids and solids at the same density and at similar temperatures. The left side of the figure contains $\langle\rho(\omega)\rangle$ for a solid just below the melting temperature, while the right side of the figure shows $\langle\rho(\omega)\rangle$ for a liquid at the same density. The top, middle, and bottom rows are for reduced densities ($\rho^*=\rho\sigma^3$) of 0.85, 0.94, and 1.0, respectively. The upper line on each panel is the full INM density of states, while the lower line shows the density of states for the zero-force INMs.

We have computed the imaginary frequency INM density of states for a solid and super-cooled liquid at identical temperatures and densities. The densities of states for these systems are shown in the upper panel of figure 4 along with a plot of the differences between the two systems. Note that the solid exhibits modes that are closer to zero while the super-cooled liquid exhibits modes at slightly higher frequencies. We have also plotted the densities of states for the imaginary-frequency double-well (DW), extended DW, localized DW, and zero-force INMs in the lower panels of the same figure. In all five of these distributions, we observe that the solid exhibits imaginary frequency modes, yet we know (from the quenches to the fcc configuration) that no barriers to diffusion are being crossed in the solid. Keyes[6] has suggested that in order to remove the non-barrier INMs from consideration in their theories, one should set a cutoff frequency which separates the high-frequency barrier crossing

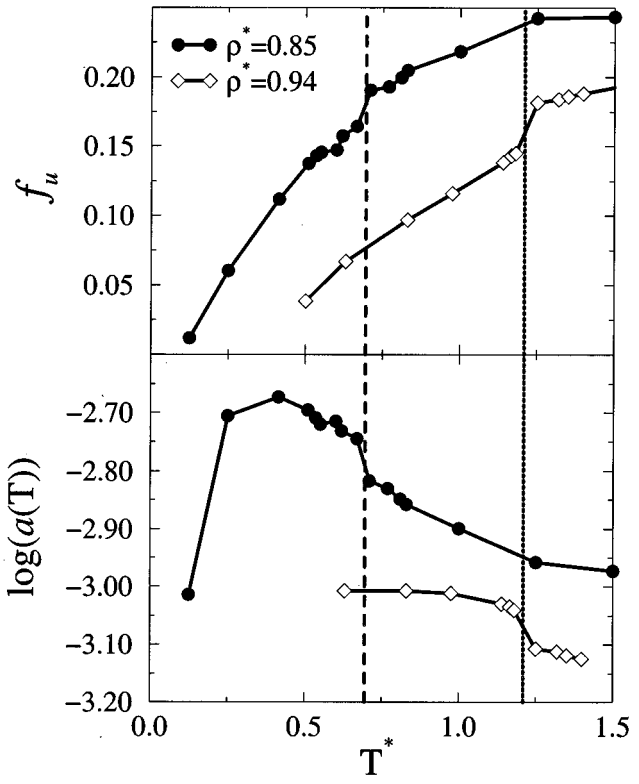

FIG. 3. The fraction of unstable normal modes shown in the upper panel and the multiplicative prefactor $a(T)$ [Eq. (11)] shown in the bottom panel for two densities plotted versus temperature. The full circles (●) are calculated at $\rho^*=0.85$ and open diamonds (◇) are calculated at $\rho^*=0.94$. The dashed and dotted lines indicate the phase transition at $T^*=0.69$, $\rho^*=0.85$ and $T^*=1.20$, $\rho^*=0.94$, respectively. Notice the discontinuities at the transition temperatures.

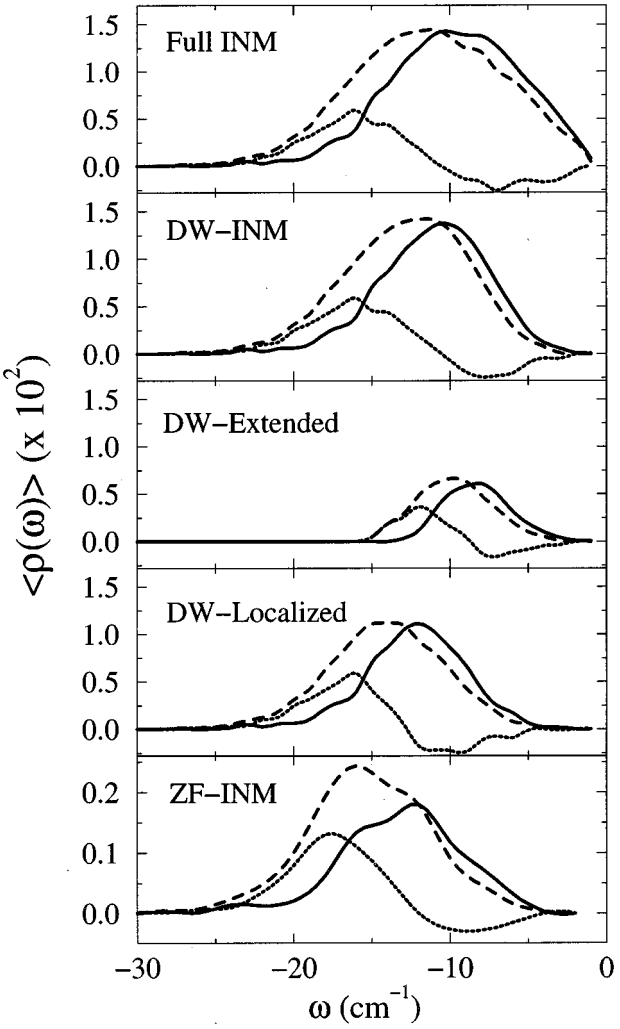

FIG. 4. Five related measures of the number of unstable modes at frequency ω for two Lennard-Jones systems at the same temperature and density ($\rho^*=0.85$, $T^*=0.6$). In each of the five panels, the solid line is for the solid, while the dashed line is for the super-cooled liquid at the same temperature. The difference between the two densities of states is shown as a dotted line. The distributions displayed are the densities of states for all INMs (top panel), for the imaginary frequency *double-well* (DW) INMs (cf. Ref. 12). The DW modes have been partitioned into localized and extended DW modes based on a participation ratio [Eq. (15)] cutoff of 0.4. The lower panel shows density of states for the imaginary *zero-force* INMs (cf. Ref. 17).

modes from the low-frequency modes that are due to anharmonicities. The densities of states shown in figure 4 would at first glance seem to confirm that the higher frequency modes are indeed more likely to be found in super-cooled liquids that are known to exhibit diffusive barrier crossing. Whether or not a frequency cutoff is really what separates diffusive barrier crossing motion from non-diffusive motion is still open for discussion, however. We will return to this point in section III.

To summarize the results of our simulations, we have seen that diffusion constants computed via the Einstein relation from very long trajectories show a substantial jump when the solid melts. We have also seen that theories that predict barriers to diffusion from the fraction of unstable modes, f_u, although they obtain a discontinuity at the melting temperature, do not reproduce a diffusion constant in the solid that is many orders of magnitude smaller than in the liquid. Using only the zero-force instantaneous normal modes as suggested in Ref. 17, the discontinuity is still much smaller than that calculated via the Einstein relation. It is apparent, then that the imaginary frequencies are not an accurate measure of the barriers to diffusion. What then gives rise to the imaginary frequency INMs in the solids? An answer to this question might point to possible methods for extracting the relevant barriers for diffusion.

III. THE ORIGIN OF IMAGINARY FREQUENCIES IN LENNARD-JONES SYSTEMS

The plots of $\langle\rho(\omega)\rangle$ for the perfect solids in figure 2 show a surprising number of instantaneous normal modes which have imaginary frequencies. At some densities, it is impossible to tell liquids from solids near the melting point simply by looking at $\langle\rho(\omega)\rangle$, even though the solid is in an fcc configuration with a translational order parameter of 0.8 (due to thermal fluctuations of the atomic positions away from their fcc lattice positions) and the liquid has an order

parameter approaching zero. LaViolette and Stillinger have also observed that there are imaginary frequency modes in solids that are at temperatures as low as one-fourth the melting temperature.[28]

The bulk of the so-called unstable INMs present in liquids survive into the solid phase, and we have seen from the evidence presented in section II that these imaginary frequencies do not correspond to diffusive barrier crossing. We would like to understand which motions lead to these imaginary frequencies with the aim of modeling diffusion using only those modes which really do cross barriers to diffusion.

We start our analysis by looking at the ''quenched'' trajectories first explored by Stillinger and Weber.[2–5] For a long trajectory, the configurations after every 10 fs were quenched to the nearest local minimum by steepest descent. If the barrier crossings really do lead to diffusion, then once a trajectory has crossed a barrier into another basin, the quenched configuration should differ from the original quenched configuration. One useful measure of the displacement in configuration space is

$$\delta q^2(t)=\sum_{i=1}^{N}(\mathbf{r}_i^q(t)-\mathbf{r}_i^q(0))^2, \tag{20}$$

where $\mathbf{r}_i^q(t)$ is the position of particle i in the configuration obtained by *quenching* the configuration at time t. Stillinger and Weber have also tried to obtain an estimate of the hopping time, τ_h, for each basin by observing the time it takes for $\delta q(t)$ to experience a jump.[3]

In the crystalline solids, despite the presence of zero-force imaginary INMs, δq is always found to be zero. This means that in the solid, the configurations *always* quench to the minimum energy fcc configuration even though the trajectory can be found at the tops of barriers quite frequently. This is an apparent contradiction. How can a trajectory that crosses barriers not be diffusing into an adjacent minimum on the potential energy surface?

The answer to this riddle can be found by looking at the instantaneous normal modes of a colinear three atom system. The potential energy contours for such a system are shown in figure 5. For configurations with $r_{12}=r_{23}>\sim 4.4$ Å, the instantaneous normal modes are the symmetric stretch (vector Q_a in figure 5) and the anti-symmetric stretch (vector Q_b). At those configurations, at least one of the normal mode frequencies (corresponding to motion along the Q_b direction) is imaginary, and the system is experiencing *no force* along that direction. Quenching the configuration on either side of the barrier leads back to the same minimum energy structure even though the trajectory has crossed a barrier!

In the configuration used to evaluate the INMs in figure 5, *both* instantaneous normal modes have imaginary frequencies. The symmetric stretch mode, Q_a, does have the equivalent to a barrier to diffusion (at infinite separation) with a barrier height of 2ϵ. If the INMs were evaluated at a different point along this mode ($r_{12}=r_{23}$), the frequency would change continuously from a positive frequency at small r to an imaginary frequency, and eventually to 0 at infinite separation. This means that the frequency along Q_a is *uncorrelated* from the real barrier height in that direction. Q_a is not a zero-force mode, however, so while it is used in predicting the diffusion constants in Keyes' theory, it would not be used in the zero-force extension.

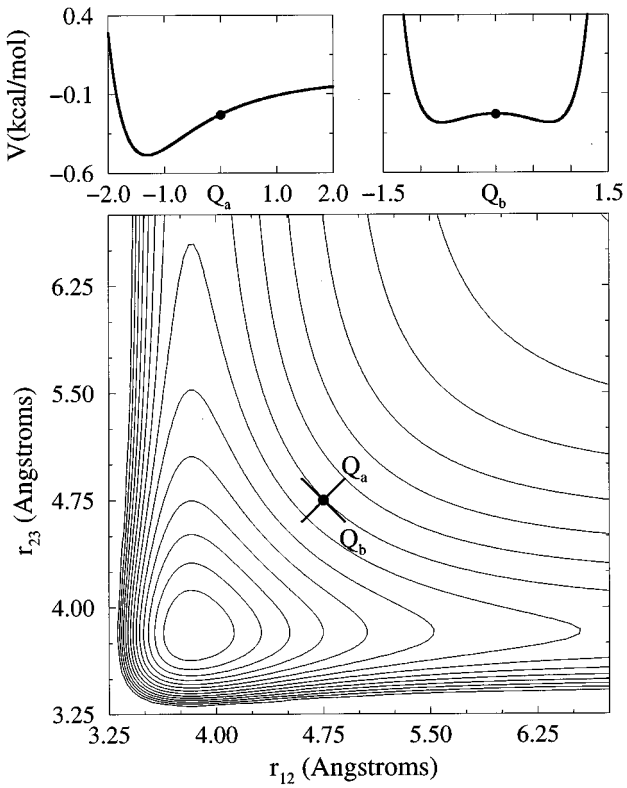

FIG. 5. A contour plot of the potential energy surface for three colinear Lennard-Jones argon atoms. (r_{ij} is the distance between atoms i and j). The instantaneous normal modes (Q_a and Q_b) have been evaluated at the point $r_{12}=r_{23}=4.75$ Å. Projections of the potential energy along these modes are shown in the upper two panels. Note that quenches from the minima on the Q_b projection will both lead to the same minimum on the surface.

Quenches from each of the two minima on the projection of the anti-symmetric stretch (Q_b) both lead back to the same minimum or basin, so the motion along Q_b is clearly not diffusive. That is, there will be no long-time separation of the atoms from their initial positions at these energies. Q_b is a zero-force mode, however, and would thus be used to predict diffusion in both versions of the theory. It is this kind of motion that we think is responsible for the confusing situation in the solids. This model system shows that there can be imaginary frequency INMs (even zero-force INMs) which do not cross diffusive barriers.

It would be reasonable to argue that these kinds of motion (imaginary modes that quench to a single minimum) don't really exist in a system with many more degrees of freedom since they require a relatively high potential energy in order to be observed. As evidence against this argument, we have plotted contours of representative (two-dimensional) potential energy surfaces that are felt by individual atoms from our simulations when all other atoms have been frozen in place. These contours are shown in figure 6. In the potential energy surfaces for the solid, super-cooled liquid, and for one of the liquid configurations, it is easy to

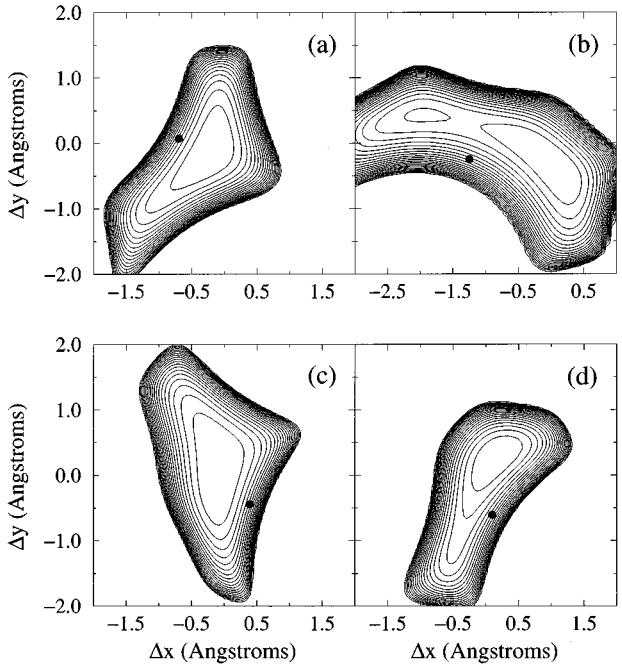

FIG. 6. Representative contour plots of the local potential energy surface felt by single atoms when all other atoms have been frozen. Panels (a) and (c) were in a super-cooled liquid and solid, respectively (both at $T^*=0.6$, $\rho^*=0.85$). Panels (b) and (d) were in liquids (both at $T^*=0.81$, $\rho^*=0.85$). The solid dots on the surfaces illustrate points on the surface with at least one zero-force imaginary mode. In panels (a), (c), and (d), quenching from either side of the dot leads to the same minimum. In panel (b), the system can quench to two different local minima, but we were only able to observe configurations like this in the liquid. The contours are 0.2 kcal/mol apart.

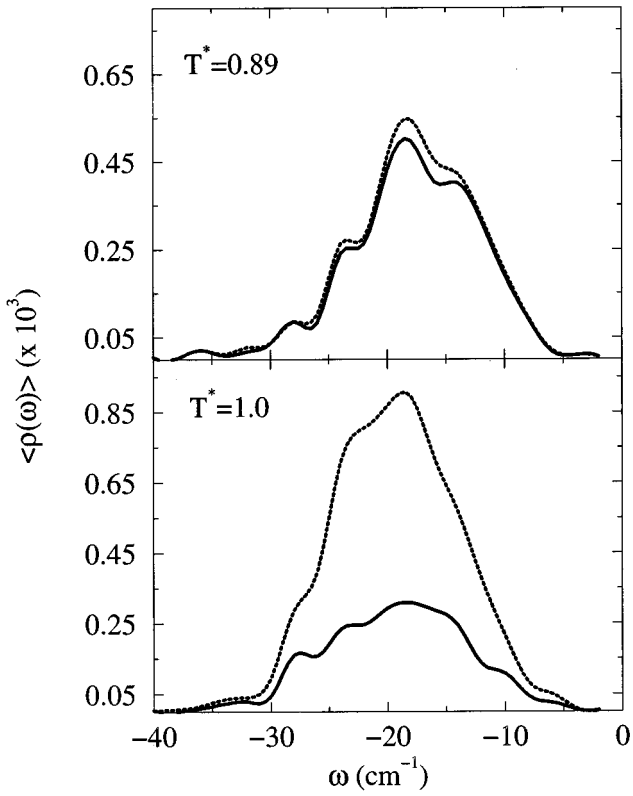

FIG. 7. The density of states for all of the imaginary frequency ZF-INMs (dotted line) and also for those which quench to the same basin from both sides of the barrier along that INM (solid line) for super-cooled liquid argon at reduced density $\rho^*=1.0$. At the lower temperature, nearly all steepest descent paths starting on either side of the barrier along the imaginary ZF-INMs lead to the same basin. This is not the case for the higher temperature, where a large fraction of the imaginary ZF-INMs do quench to separate basins. As expected, the density of ZF-INMs is shifted to higher imaginary frequencies at higher temperatures.

see that there are regions with imaginary frequency that will all quench to the same minimum on the potential surface. On each of these surfaces, we have used a dot to indicate a configuration which has an imaginary *zero-force* mode. In the liquid, we were also able to find surfaces where configurations on either side of a zero-force mode (on this reduced surface) could quench to different minima. We were not able to find any of these surfaces in the solid configurations. Also evident in figure 6 is the rather low energy gap between the locations of the zero-force modes (indicated with dots) and the local minima. This implies that for systems with many degrees of freedom the motions described in figure 5 are even more accessible. Moreover, when all the atoms are moving, this energy gap can even decrease.

The question remains which of the imaginary frequency INMs in the *liquids* describe saddles that connect two *different* basins with respect to diffusion. In order to answer this question we have classified the imaginary ZF-INMs according to the fate of the steepest descent path. If the quenches from both sides of the barrier along a given imaginary frequency ZF-INM result in the same configuration, then that mode is said to exhibit the ''false-barrier phenomenon.'' If the two quenched configurations differ, that imaginary frequency ZF-INM is somewhere near a ''real'' barrier. Figure 7 shows the full imaginary frequency ZF-INM density of states and also the fraction of ZF-INMs which exhibit the false barrier phenomenon. The simulations were done for a super-cooled liquid at a reduced density $\rho^*=1.0$, a density for which the Zwanzig model is thought to be correct. (In lower density liquids, the Zwanzig picture of basin hopping begins to break down, which makes this kind of analysis meaningless.) The most unexpected result is that almost all the saddles predicted from the imaginary ZF-INMs at $T^*=0.89$ do not connect different basins. In the colder super-cooled liquid, almost all of the barriers are false, just as they were in the solids at lower density.

At a somewhat higher temperature, there are still a considerable number of false barriers. Also evident in figure 7 is the wide frequency range over which the false barriers are in evidence. There is no cutoff frequency (as suggested by Keyes[6]) which would allow one to easily separate the false barriers from those imaginary frequency INMs which are close to real barriers.

Straub *et al.* have suggested that the cutoff should be in the *height* of the barrier rather than the *frequency*.[16] This suggestion differs from the previous one only when the barrier heights are not correlated with the frequencies. We do not see any reason to suspect that the false barrier problem

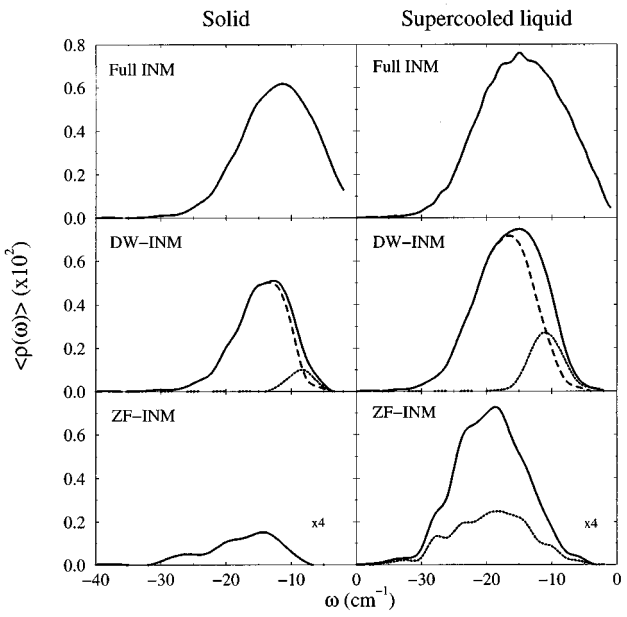

FIG. 8. A complete analysis of the instantaneous normal modes (INMs) for solid and super-cooled liquid argon (both at $\rho^*=1.0$, $T^*=1.0$). The upper panels show the densities of states for all of the imaginary frequency INMs. In the middle panels, the imaginary frequency double-well (DW-INM) densities are shown (solid lines) and are segregated into ''local'' (dashed lines) and ''extended'' (dotted lines) modes. The lower panels show the imaginary frequency zero-force (ZF-INM) densities (solid lines). The densities of states for the *false-barrier* zero-force INMs are shown with a dotted line in the bottom panel. Note that *all* of the modes in the solid are false-barrier modes.

would not persist into the higher energy regime. (The problem exists at a wide range of barrier heights in figure 5, for example.) Most importantly, this suggestion seems to argue against the main point of the original INM theories — if barrier heights are uncorrelated with the local frequency at the top of the barrier, then a theory based on a local expansion of the surface can give no meaningful information about transition state theory rates.

The disappearance of the INMs which are near true barrier regions with decreasing temperature might explain the plateau regime observed in the multiplicative prefactor $a(T)$, seen in figure 3 for lower densities. Keyes[6] has also observed this plateau regime at reduced density $\rho^*=1.0$. We believe that this plateau regime is indicative of super-cooled liquids in which most (if not all) of the imaginary frequency INMs exhibit the false barrier phenomenon.

A complete picture of the density of states of imaginary frequency INMs in each of the distributions is shown in figure 8. These modes were calculated from 500 atom simulations done at $\rho^*=1.0$, $T^*=1.0$. Each mode was examined to determine if it was a double-well (DW) mode, and DW modes were segregated into ''local'' and ''extended'' DW modes using a participation ratio [Eq. (15)] cutoff of 0.4, which is known to be the correct cutoff for this density and number of particles.[12] Additionally, modes that met the zero-force criterion were quenched on either side of the barrier to determine if that mode did indeed lead to a different local minimum on the potential energy surface. (To save CPU time, quenching was done for modes in the 108 particle systems.) Those modes that lead to the same local minimum were counted as false barrier modes.

We can see from the distribution of false barrier modes (in both the super-cooled liquid and solid), that none of the distributions proposed to date will remove all of the false barrier modes from the solid, and that many of the false barrier modes persist into the super-cooled liquid. Bembenek and Laird have observed that the extended DW modes disappear at the glass transition temperature,[12] and Sciortino and Tartaglia have recently observed that *all* of the DW modes disappear at T_g in super-cooled water,[29] but we do not observe a similar phenomenon at the melting transition.

In summary, we believe that the imaginary frequency INMs observed in the solid are simply a measure of the anharmonicities on the potential energy surface and do not correlate with the barrier heights of a diffusive process. The fact that a simple three atom system can experience an imaginary frequency zero-force INM while still quenching to a single minimum argues strongly that this kind of motion is the source of these modes on the potential energy surface for a much larger system of Lennard-Jones particles. In the solids, we have observed exactly this behavior (imaginary frequency zero-force INMs which quench to a single minimum). Liquids traverse the same potential energy surface, and while we have not proven that this kind of motion is responsible for the imaginary frequency INMs in the liquids at all densities, it is clearly true for super-cooled liquid argon at $\rho^*=1.0$.

We have seen that individual atoms can also experience configurations on the local potential energy surface that exhibit the same kind of behavior (imaginary frequency zero-force INMs which quench to a single minimum). These were observed in the solids, as well as in the super-cooled and regular liquids. Since these modes are used to predict barrier crossing rates in both versions of the INM theory, we feel that in their current form, diffusion constants calculated via these theories have only accidental agreement with the actual diffusion constants in the liquids.

IV. CONCLUSION

We believe that the evidence presented above argues against the use of local information on the potential energy surface (the INM frequencies) to predict dynamical properties like the diffusion constant. Our arguments against the use of the INM frequencies for this purpose can be summarized as follows:

(1) The diffusion constants predicted from INM and zero-force INM densities of states for the solids are incorrect. Although Keyes specifically warns against using them for solids,[6] there is no *a priori* way to identify the phase of matter from the INM density of states. This certainly limits the predictive power of the theory.
(2) It is possible that the wells on either side of imaginary zero-force INMs can quench to the same local minimum on the surface. This is certainly true for model systems like the colinear three atom system in figure 5 and may

be generally true of the full potential energy surface for a larger system of Lennard-Jones particles. The solids observed in section II visit low-energy regions of the potential energy surface, and quenches from both sides of imaginary frequency zero-force INMs lead to the fcc structure. High-density super-cooled liquids also display many modes with false barriers. Although higher-temperature liquids can visit a larger fraction of the potential energy surface, the surface itself is now known to have regions for which the imaginary frequency INMs are not accurate predictors of the barriers to diffusion.

(3) Even though the solids we studied exhibited imaginary zero-force INM frequencies, they always quenched to the fcc configuration. Even the modes for a single atom in the solid (cf. figure 6) never displayed another energetically accessible local minimum. We were able to find atoms with two available local minima in the liquid, however.

(4) In some model systems, the imaginary INM frequency along the modes *with* barriers to diffusion (e.g., Q_a in figure 5) are found to be uncorrelated with the barrier height.

(5) The differences between f_u and $a(T)$ in the liquids and solids are slight (cf. figure 3) and cannot account for a many orders-of-magnitude jump in the diffusion constant.

We conclude (with some disappointment) that the INM models for the diffusion constant presented so far rest on the untenable assumption that the imaginary frequency instantaneous normal modes are indicators of barrier crossings of the *same type* that lead to diffusive motion. It may be possible to use the kind of approach suggested by Keyes if a method is developed which is able to discriminate between the modes which really are crossing the barriers to diffusion from those which are not. The methods that have already been suggested for this purpose (frequency cutoffs or using only the double-well, extended double-well, or zero-force INMs) have all been shown to admit modes which have false barriers in the high-density super-cooled liquids and solids. We have suggested a way to eliminate modes that have false barriers by following the steepest descent path from either side of an imaginary frequency INM to the nearest local minimum. However, this approach is limited to high-density super-cooled liquids and solids and does not guarantee that all of the imaginary modes which remain are indeed crossing barriers to diffusion.

Finally, we note that our investigations have been limited to atomic systems, and that the situation may be more complex for molecular liquids. Given the results presented in this paper, it is important to establish for molecular solids whether or not imaginary frequency instantaneous normal modes are simply indicators of false barriers, anharmonicities, and surface convexities as they appear to be in the Lennard-Jones solids.

ACKNOWLEDGMENTS

The authors would like to acknowledge helpful discussions with Professors T. Keyes and J. Straub. This work was supported by a grant from the National Science Foundation. ER is a Rothschild and Fulbright post-doctoral fellow.

[1] R. Zwanzig, J. Chem. Phys. **79**, 4507 (1983).
[2] F. H. Stillinger and T. A. Weber, Phys. Rev. A **25**, 978 (1982).
[3] F. H. Stillinger and T. A. Weber, Phys. Rev. A **28**, 2408 (1983).
[4] T. A. Weber and F. H. Stillinger, J. Chem. Phys. **80**, 2742 (1984).
[5] F. H. Stillinger and T. A. Weber, J. Chem. Phys. **83**, 4767 (1985).
[6] T. Keyes, J. Chem. Phys. **101**, 5081 (1994).
[7] T. Keyes, J. Chem. Phys. **104**, 9349 (1996).
[8] T. Keyes, J. Chem. Phys. **106**, 46 (1997).
[9] M. Cho, G. R. Gleming, S. Saito, I. Ohmine, and R. M. Stratt, J. Chem. Phys. **100**, 6672 (1994).
[10] G. Goodyear, R. E. Larsen, and R. M. Stratt, Phys. Rev. Lett. **76**, 243 (1996).
[11] S. D. Bembenek and B. B. Laird, Phys. Rev. Lett. **74**, 936 (1995).
[12] S. D. Bembenek and B. B. Laird, J. Chem. Phys. **104**, 5199 (1996).
[13] J. E. Adams and R. M. Stratt, J. Chem. Phys. **93**, 1332 (1990).
[14] J. E. Adams and R. M. Stratt, J. Chem. Phys. **93**, 1632 (1990).
[15] J. E. Straub and J. K. Choi, J. Phys. Chem. **98**, 10978 (1994).
[16] J. E. Straub, A. B. Rashkin, and D. Thirumalai, J. Am. Chem. Soc. **116**, 2049 (1994).
[17] G. V. Vijayadamodar and A. Nitzan, J. Chem. Phys. **103**, 2169 (1995).
[18] B. Madan and T. Keyes, J. Chem. Phys. **98**, 3342 (1993).
[19] T. Wu and R. F. Loring, J. Chem. Phys. **97**, 8568 (1992).
[20] D. J. Isbister and D. A. McQuarrie, J. Chem. Phys. **56**, 736 (1972).
[21] S. A. Egorov, M. D. Stephens, A. Yethiraj, and J. L. Skinner, Mol. Phys. **88**, 477 (1996).
[22] G. D. Harp and B. J. Berne, Phys. Rev. A **2**, 975 (1970).
[23] D. C. Douglass, J. Chem. Phys. **35**, 81 (1961).
[24] B. J. Berne and G. D. Harp, Adv. Chem. Phys. **17**, 63 (1970).
[25] B. J. Berne and R. Pecora, *Dynamic Light Scattering* (Krieger, Malabar, FL, 1990).
[26] M. P. Allen and D. J. Tildesley, *Computer Simulation of Liquids* (Oxford University Press, Oxford, 1987).
[27] G. C. Maitland, M. Rigby, E. B. Smith, and W. A. Wakeham, *Intermolecular Forces: Their Origin and Determination* (Clarendon, Oxford, 1981).
[28] R. A. LaViolette and F. H. Stillinger, J. Chem. Phys. **83**, 4079 (1985).
[29] F. Sciortino and P. Tartaglia, Phys. Rev. Lett. **78**, 2385 (1997).